Sensors & Transducers, Vol. 259, Issue 5, October 2022, pp. 99-108

www.sensorsportal.com

Sensors & Transducers

Published by IFSA Publishing, S. L., 2019
http://www.sensorsportal.com

Towards Selective and Sensitive Detection of Carbon Monoxide with CuO/ZnO Heterojunction Nanocomposite Prepared by an Organometallic Approach

[1, *] Justyna Jońca, [2] Katia Fajerwerg, [2] Myrtil L. Kahn, [3] Philippe Menini, [1] Izabela Sówka and [2, 4, *] Pierre Fau

[1] Wroclaw University of Science and Technology, Faculty of Environmental Engineering, Department of Environment Protection Engineering, Wybrzeże Wyspiańskiego 27, 50-370 Wrocław, Poland
[2] Laboratoire de Chimie de Coordination, LCC-CNRS, Université de Toulouse, 205 Route de Narbonne, BP 44099, 31077 Toulouse cedex 4, France
[3] Laboratoire d'Analyse et d'Architecture des Systèmes, Université de Toulouse, CNRS, UPS, 7 Av. du Colonel Roche, 31400 Toulouse, France
[4] Laboratoire de Physique et Chimie de Nano-Objets, LPCNO-INSA, Université de Toulouse, 135 Avenue de Rangueil – INSA, 31077 Toulouse Cedex 4, France
[*] E-mail: justyna.jonca@pwr.edu.pl, pfau@insa-toulouse.fr

Received: 5 September 2022 Accepted: 10 October 2022 Published: 31 October 2022

Abstract: Nanometer size p-n heterojunction has been created from CuO and ZnO anisotropic nanoparticles prepared by a one-pot organometallic approach. The method is based on the hydrolysis or oxidation of an adequate metal-organic precursors in pure octylamine. The CuO and ZnO nanostructures were dispersed in ethanol and then, mixed at different mass ratios, *i.e.* CuO(75%)/ZnO(25%), CuO(50%)/ZnO(50%) and CuO(25%)/ZnO(75%). Finally, the CuO and ZnO suspensions and their mixtures were deposited on miniaturized gas sensors substrates by an ink-jet printing method and heated up gradually to 550 °C in ambient air. Then, the as-prepared sensors have been exposed to CO (100 ppm), C_3H_8 (100 ppm) and NH_3 (5 ppm) at different working temperatures (from 75 °C to 400 °C) and under 50 % of relative humidity (RH). Among all prepared sensors the one based on the mixture of CuO (75 %) and ZnO (25 %) presents a very sensitive and selective response to CO. Indeed, at the operating temperature of 165 °C, a high sensitivity towards CO was obtained (S_{CO}=624 %). In these conditions, the sensor exhibited low sensitivity to other tested gases ($K_{CO/C3H8}$= 14.5 and $K_{CO/NH3}$= 26) but its response time was quite long (t_{90}=2.3 min) and the recovery was very sluggish (t_{10}> 20 min). Therefore, it was better to increase the working temperature up to 300 °C. Although the sensitivity and selectivity towards CO worsened (S_{CO}=177%, $K_{CO/C3H8}$= 4.7 and $K_{CO/NH3}$= 9.8) the response/recovery time decreased to 50 s/4.5 min. The gas sensing performances of the CuO(75%)/ZnO(25%) composite was attributed to both high surface to volume ratio of the prepared nanostructures and the p-n heterojunction established between the CuO and ZnO nanoparticles.

Keywords: Organometallic approach, CuO/ZnO nanocomposite, Heterojunction, MOS gas sensors.

1. Introduction

The use of miniaturized gas sensors is of increasing interest in areas such as environmental monitoring, safety, medical diagnostics and agriculture [1]. Metal oxide semiconductor gas sensors (MOS) are the most popular choice for these applications due to their numerous advantages, *i.e.* long lifetime, low cost,

small size and short response time. However, these devices have their limitations as well. They exhibit baseline drift, sensor poisoning, poor selectivity and low manufacturing reproducibility [2, 3]. Although much has been done in order to deal with these problems, the improvement of MOS sensors continues to attract researchers' attention.

The performance of MOS sensors is influenced by various parameters including: design of the sensing platform (*e.g.* geometry of electrodes and heating element), device operating temperature and physical and chemical properties of the sensing materials (*e.g.* grain size, defects density and presence of oxygen vacancies). The improvement of gas sensing properties of metal oxide semiconductors can be accomplished by designing them at the nanoscale [4]. Therefore, the synthesis of nanoparticles has attracted considerable interest. In comparison with high temperature vapor phase deposition method, solution-based chemistry protocols can be conducted at mild temperature and offer additional advantages such as straightforward processing, low cost, and eases of scale up. Among them, the organometallic approach, developed at the Laboratoire de Chimie de Coordination (LCC-CNRS), leads to well-controlled nanostructures in terms of size dispersion, chemical composition, surface chemistry properties, shape or organization [5]. Indeed, hydrolysis or oxidation of metal-organic precursors in the presence of alkylamine ligands produced several well-defined nanostructures of metal oxides by a one-step procedure [6-9]. Among them, the ZnO, CuO and SnO_2 nanoparticles were used for gas sensing applications [7-9]. For example, Ryzhikov et al., [7] investigated the ZnO morphology influence on the sensor response towards CO, C_3H_8 and NH_3 gases. More in details ZnO anisotropic nanoparticles, isotropic nanoparticles and cloudy-like aggregates were investigated as gas sensing layers. Sensors prepared with the anisotropic nanoparticles showed the highest response to both CO and C_3H_8, whereas sensors based on cloudy-like structures show the weakest response to C_3H_8. No effect of the ZnO morphology has been evidenced for NH_3 gas. It was concluded that the differences in sensors performance must be correlated to the exposed crystalline faces and their reactivity to the target molecules.

The dimensionality of the nanostructure can also have a significant impact on sensor response. For example, Jońca et al. [9] formed SnO_2 nanoparticles (0D structure) and hierarchical structures resembling a regular octahedron (3D structure) made of assembly of these nanoparticles. When exposed to low concentrations of CO (*i.e.* 0.25 to 20 ppm), hierarchical structures showed greater sensitivity than SnO_2 nanoparticles, but exhibited a lower upper limit of detection (*i.e.* 100 ppm *vs*. 500 ppm).

Gas sensing properties of metal oxide nanoparticles can be further improved by their decoration with noble metals or by doping them with 2D materials (*e.g.* graphene, g-C_3N_4, MoS_2, black phosphorus, etc.) [10]. Another approach is to combine two metal oxides in order to create a heterojunction [11]. Heterojunction refers to the area at the interface between two semiconductors with different band gap values. Due to the different chemical and physical parameters of both materials (*i.e.* band structure, dielectric constant, lattice constant, electron affinity), the phenomenon of mismatch at the interface gives the heterojunction new properties, which can find application, among others, in the construction of gas sensors.

MOS can be divided into two types, *i.e.* p-type (electron-hole concentration > free electron concentration, *e.g.* CuO, NiO, Fe_2O_3) and n-type (free electron concentration > electron-hole concentration, *e.g.* ZnO, WO_3, SnO_2). Therefore, three kinds of heterojunction can be distinguished: n-n, p-p and p-n. The gas sensing properties of the p-n heterojunction, including the CuO/ZnO one, have been explored by many research groups. Indeed, several CuO/ZnO-based gas sensors were prepared for the detection of HCHO, C_3H_6O, C_2H_5OH, NO_2, CO_2, H_2S, NH_3, etc. [12-18]. These sensors exhibited higher sensitivity, better selectivity and shorter response/recovery times than the devices based on single oxides. At the same time, it was found that the mass ratio of oxides used for the sensitive layer preparation plays a crucial role on the sensor performance. Moreover, mentioned above ZnO/CuO based sensors were operated at relatively low temperatures (some of them at room temperature) and thus, are suitable candidates to fulfill the market demand for near-zero power consumption devices.

This work explores gas sensing properties of the p-n heterojunction based on CuO and ZnO anisotropic nanoparticles prepared by the organometallic approach [6, 7]. The CuO and ZnO nanoparticle suspensions and their mixtures were evaluated as gas sensitive layers. These sensors have been exposed to different gaseous mixtures, *i.e.* 100 ppm CO, 100 ppm C_3H_8 and 5 ppm NH_3 at different working temperatures (from 75 ºC up to 400 ºC) under 50 % of relative humidity (RH). The optimal gas sensing performances were achieved for the CuO(75%)/ZnO(25%) configuration. Remarkably, in the case of CO detection, S_{CO}= 177%, $K_{CO/C3H8}$= 4.7 and $K_{CO/NH3}$= 9.8 and a response/recovery time of 4.5 min is obtained at 300 °C. The enhanced gas sensing properties of the CuO(75%)/ZnO(25%) sensors was attributed to the p-n heterojunction between the CuO and ZnO grains. The gas sensing mechanism of the mentioned heterojunction is also proposed herein.

2. Materials and Methods

2.1. Nanoparticles Synthesis

CuO nanoparticles (CuO Nps) were obtained from a mixture of (N,N'-diisopropylacetamidinato) Copper (I) (Cu(iPr-Me-amd)]$_2$) (0.125 mmol, 51 mg) and octylamine (0.625 mmol, 80.5 mg). Reagents were mixed in a small glass vial and then exposed to

ambient atmosphere. After 16 h, the obtained black product was washed 3 times with 5 mL of acetone using centrifuge (5000 rpm, 25 °C, 5 min).

ZnO nanoparticles (ZnO NPs) were obtained from a mixture of ($Zn(c\text{-}C_6H_{11})_2$ (0.25 mmol, 57.9 mg) and octylamine (0.5 mmol, 65 mg). The reagents were also prepared in a small glass vial, but then placed in a flat-bottomed reactor at room temperature and under argon atmosphere. The hydrolysis was performed by addition of degassed water to the reactor (18 µL). After 4 days, the obtained white product was washed one time with 5 mL THF and 3 times with 5 mL of acetone and centrifuge at 5000 rpm, 25 °C during 5 min.

2.2. Characterization

A JEOL JSM 1011 Transmission Electron Microscope (TEM) operating at 100 kV was used forimaging. TEM specimens were prepared by drop deposition of the washed and dispersed in ethanol nanomaterials on a carbon-supported copper or nickel grids. Analysis of the images were performed using Digital Micrograph program with at least 100 nanoparticles. The powder-diffraction patterns were obtained using SEIFERT XRD 3000TT X-Ray Diffractometer with Cu-Kα radiation, fitted with a diffracted-beam graphite monochromator. The data were collected in the 2θ configuration between 20 and 80°.

2.3. Gas Sensor Preparation

Freshly prepared and washed ZnO and CuO nanostructures were dispersed in ethanol. The concentration of the nanostructures in the solution was 5 $mg.mL^{-1}$. From these two solutions, mixtures of ZnO/CuO were prepared at different mass ratios: CuO(75%)/ZnO(25%), CuO(50%)/ZnO(50%), CuO(25%)/ZnO (75%). Finally, the CuO and ZnO suspensions and their mixtures were deposited on miniaturized gas sensors substrates by an ink-jet printing method (Microdrop AG) [19, 20].

The silicon platform of this study has been developed by the Laboratoire d'Analyse et d'Architecture des Systèmes, LAAS-CNRS. The die size is 2×2 mm^2, and it integrates a 1.4 µm thick dielectric membrane (SiO_2/SiNx/) designed for an optimized mechanical behavior and thermal insulation of the heated area. A spiral shaped platinum heater is buried between the bottom dielectric membrane and the passivation top layer (silicon dioxide). This heater structure can stand temperatures up to 700 °C and the power consumption does not exceed 55 mW at the operating temperature of 500 °C. The interdigitated platinum electrodes for the measure of the sensitive layer are deposited as a final step on the top of the SiO_2 passivation layer and present a rounded shape. A distance of 10 µm between each electrode pole provides a reliable contact even for high resistive sensing layers [20].

2.4. Gas Test set-up

Gas tests have been performed using a setup composed of different gas bottles connected to mass flow controllers (QualiFlow) commanded by an Agilent Data Acquisition/Switch Unit 34970A. Sensors are placed in a measurement cell equipped with humidity and temperature sensors. The integrated heaters are driven by a HP6642A voltage controller. A National Instruments 6035E electronic card establishes the connection between a computing unit and the measurement cell. Freshly prepared sensitive layers were initially conditioned by a sequential *in situ* heating of the sensitive layer from ambient temperature up to 550 °C in air. Afterwards, the sensitive layer resistance is stabilized on the device by annealing at 500 °C in synthetic air (relative humidity, RH 50 %) at a total gas flow rate of $1L.min^{-1}$. Finally, the sensors were exposed to controlled levels of CO, C_3H_8 and NH_3. The tests reported herein have been performed at different operating temperatures from 75 °C up to 400 °C, at 50 % RH. Resistance is measured before (R_{air}) and after (R_{gas}) sensor exposure to reducing gas mixture, and the normalized responses to given gas, $S(\%)_i$, is calculated using equation (1):

$$S_i = \frac{\left|\left(R_{air} - R_{gas}\right)\right|}{R_{air}} \cdot 100\ \%, \quad (1)$$

The selectivity coefficient, $K_{i/j}$, is expressed as the ratio between the sensor normalized responses towards investigated gases (S_i, S_j):

$$K_{i/j} = \frac{S_i}{S_j} \quad (2)$$

The response time is the time required for the sensor to reach a stable resistance value when it has been exposed to the target gas. The response time is given here as the time required to reach 90 % of the maximum signal value (t_{90}) obtained after exposure to a target gas. The recovery time, in turn, is the time necessary for the resistance to return to the value that the sensor had prior to an exposure to the target gas and is given here as the time required to achieve a resistance that is about 10% higher than the starting resistance (t_{10}). Results reported here have been performed by using at least 3 sensors prepared as described above.

3. Results and Discussion

3.1. Morphology and Chemical Composition

Detailed characterization of the CuO and ZnO NPs has been reported earlier [7, 8]. Therefore, only a brief description of the morphology and chemical composition of the mentioned materials will be provided in this manuscript.

The X-ray diffraction analyses of as-prepared and washed ZnO nanostructures are presented in Fig. 1a [7]. The hydrolysis of the zinc precursor in the presence of octylamine and under argon atmosphere led to the formation of the hexagonal zincite structure (JCPDS 26-1451). The sharp and high intensity diffraction peak at $2\theta = 34.6°$ corresponds to the (002) plane and is characteristic of the growth along the *c*-axis of the zincite crystals. The average crystallite size values, calculated by the Debye-Sherrer formula, are around 5 nm for the transversal axis and around 26 nm for the longitudinal one [7]. These results are in accordance with the TEM images analyses which depicted presence of anisotropic nanoparticles with the diameter of 5.3 ± 0.8 nm and length of 21.5 ± 5.6 nm [7] (Fig. 2a).

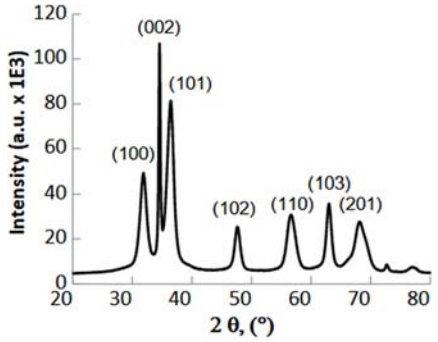

(a)

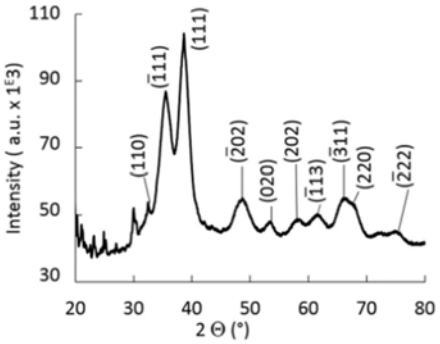

(b)

Fig. 1. X-rays diffractograms of ZnO (a) and CuO (b) nanoparticles [7, 8].

As revealed by the X-ray diffraction analyses (Fig. 1b), the oxidation of copper precursor under ambient atmosphere led to the formation of the CuO tenorite structure (ICDD: 96-410-5683) [8]. Determination of the crystallite size using Debye-Scherrer equation gives values of ca. 4–5 nm whereas the TEM images show the formation of rather anisotropic nanoparticles with uneven distribution of their size and shape (Fig. 2b). Analysis of these images through a 2D-plot representation revealed that three CuO populations of different size can be distinguished [21]. The first one, accounting for 50 % of the population, have an average width of 4.6±1.5 nm and length of 6.8 ± 2.7 nm. The second population possesses an average width of 5.8 ± 2.3 nm and length of 8.9 ± 3.5 nm and accounts for 43%. Finally, the third population, accounting for 6%, presents an average width of 6.5 ± 4.4 nm and length of 15.1 ± 10.0 nm [8]. The uneven distribution of the size and shape of the CuO NPs is probably associated with their growth conditions. Indeed, their synthesis is performed in ambient air and therefore the reaction parameters are not as well controlled as in the case of ZnO NPs.

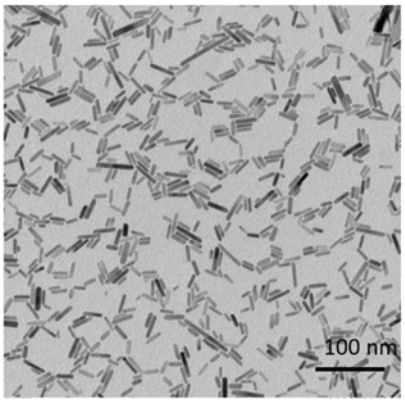

(a)

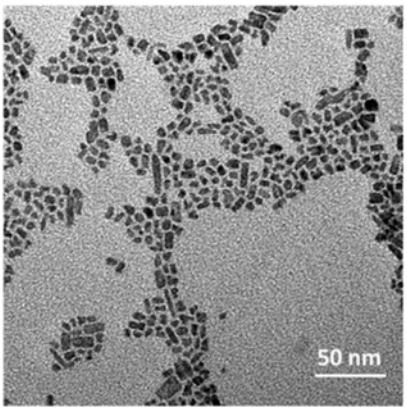

(b)

Fig. 2. TEM images of freshly prepared and washed ZnO (a), and CuO (b) nanoparticles [7, 8].

3.2. Gas Sensing Properties

Our previous studies showed that from all ZnO nanostructures prepared through the organometallic approach, the anisotropic nanoparticles exhibited the highest sensitivity towards investigated gases at high temperatures [7], whereas CuO NPs gave high selectivity and sensitivity towards CO at low temperatures [8]. In order, to further improve the performance of our sensors, we investigate in the present work the behavior of sensitive layers composed of a mixture of both nanostructures.

The CuO, ZnO NPs and their mixtures have been deposited by an ink-jet printing method as gas

sensitive layers on silicon gas sensing devices. After deposition, the layers have been *in situ* annealed by operating the integrated Pt heater up to 550°C. This step allows the slow removal of solvent and ligand traces from the washed nanoparticles. The SEM images of these layers are presented Fig. 3. Good quality metal oxide semiconductor layers without large cracks or delamination were obtained. The morphology of the nanoparticles is preserved even after this treatment.

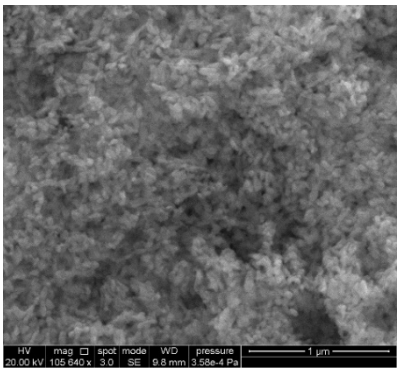

(a)

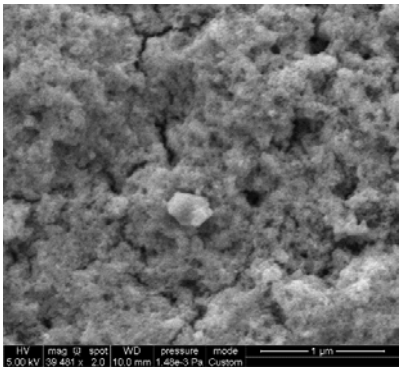

(b)

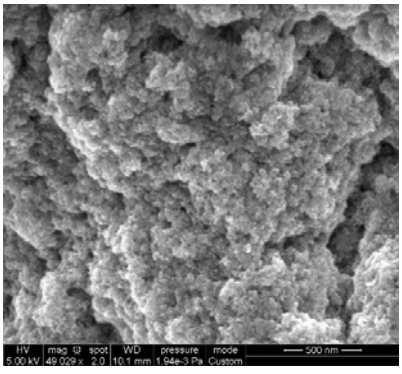

(c)

Fig. 3. SEM images of the ZnO (a), CuO (b) and CuO(50%)/ZnO(50%) (c) layers of the gas sensor devices.

In air, the CuO sensors exhibit a resistance of few kOhms. This value increases with the content of added ZnO, to reach MOhms for pure ZnO sensitive layers (Table 1). This is due to the differences in the band gap energies between these two materials, *i.e.* 1.2 eV and 3.7 eV for CuO and ZnO, respectively [22, 23]. In the presence of reducing gases, the resistance of CuO and CuO-ZnO based sensors increases which is characteristic for sensors based on p-type semiconductors. On the other hand, the resistance of ZnO based sensors decreases which is characteristic for n-type semi-conductors.

Normalized responses of all investigated sensors towards 100 ppm CO, 100 ppm C_3H_8 and 5 ppm NH_3 (RH=50 %) at different operating temperatures are presented in Fig. 4. The sensitivity of the ZnO sensor towards all investigated gases increases with the temperature, reaching the highest values at 400 °C. The highest sensitivity for the CuO sensor was achieved at 165 °C, but only towards 100 ppm CO and 100 ppm C_3H_8. The CuO sensor was not sensitive to 5 ppm NH_3 at all. This is in accordance with the results achieved earlier [7, 8]. Concerning the CuO-ZnO sensors, the highest sensitivity was also noticed at 165 °C for all tested gases and regardless the investigated metal oxide mixture. Overall, the sensitivity increases also with the CuO mass content in the sensing layer. However, for the CuO(75%)/ZnO(25%) sensor, the sensitivity is significantly higher, especially towards 100 ppm CO. This is due to the p-n heterojunction established between the CuO and ZnO NPs (Section 3.3).

From all investigated metal oxide mixtures, the CuO(25%)/ZnO(75%) sensor exhibited the lowest sensitivity. Interestingly, in the 340 °C – 400 °C temperature range, a switch from the p-type to n-type sensing behavior was observed (see Section 3.3).

Overall, the CuO(75%)/ZnO(25%) sensor is a suitable candidate for sensitive and selective CO detection. Indeed, the highest sensitivity towards 100 ppm of CO was achieved with sensitive layers composed of CuO (75 %) and ZnO (25 %) when operated at 165 °C, *i.e.* S_{CO} = 624 % (Table 2).

Moreover, the sensor showed relatively low response to 100 ppm C_3H_8 and 5 ppm NH_3, which indicates its high selectivity towards CO in these conditions ($K_{CO/C3H8}$=14.5 and $K_{CO/NH3}$=26). Therefore, the sensitivity and $K_{CO/C3H8}$ coefficient were improved as compared to ZnO (R_{CO}=39 % and K_{CO}/K_{C3H8}=1.2 at 400 °C) and CuO (S_{CO}=227 %, $K_{CO/C3H8}$=11.2 at 165 °C) sensors at their optimal operating temperatures (Table 2).

Table 1. The resistance (kOhm) of the ZnO, CuO and ZnO/CuO gas sensors at different operating temperatures.

T °C	CuO	CuO/ZnO (75%/25%)	CuO/ZnO (75%/25%)	CuO/ZnO (75%/25%)	ZnO
400	1.20	3.55	845	1094	3603
340	1.29	3.96	982	1921	4438
300	1.42	4.68	1326	2945	4626
165	2.44	17.8	4712	10366	9742
75	13.3	230	19547	22389	87341

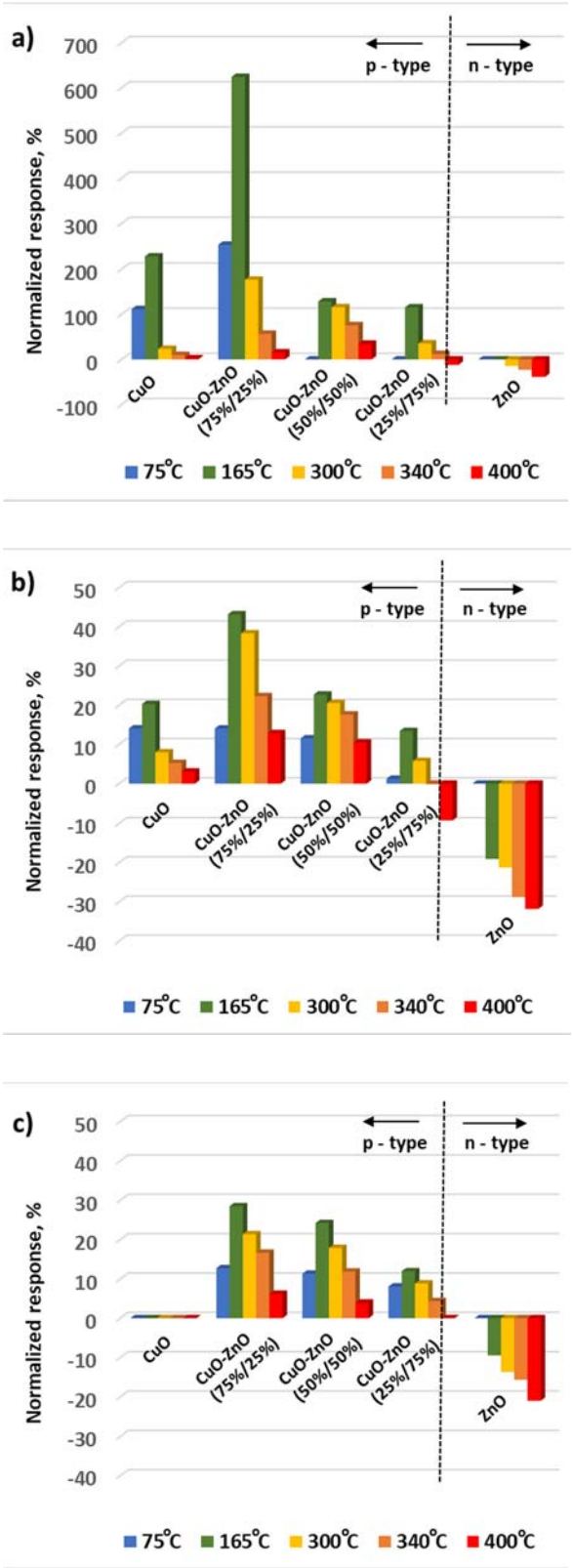

Fig. 4. Normalized response of the CuO, ZnO, and CuO/ZnO based gas sensors towards 100 ppm CO (a), 100 ppm C_3H_8 (b) and 5 ppm NH_3 (c) at different operating temperatures (50 % RH). The gas responses at 75°C present a very slow response time and the normalized response is measured before the complete resistance variation is reached, this value is therefore a transitory one and is under-evaluated. Please note, that the scale at (a) is different from the scale at (b) and (c).

Table 2. The normalized response (S_{CO}), selectivity coefficients ($K_{CO/C3H8}$ and $K_{CO/NH3}$), response (t_{90}) and recovery time (t_{10}) for the ZnO, CuO and CuO(75%)/ZnO(25%) gas sensor towards 100 ppm CO at different operating temperatures.

T, °C	S_{CO}, %	$K_{CO/C3H8}$	$K_{CO/NH3}$	t_{90}	t_{10}
CuO MOS sensor					
75*	111.4	7.9	selective	> 20 min	> 20 min
165	226.7	11.2	selective	6.2 min	20 min
300	23.4	2.9	selective	20 s	2 min
340	9.9	1.9	selective	30 s	30 s
400	2.5	0.8	selective	59 s	30 s
CuO(75%)/ZnO(25%) MOS sensor					
75*	252.7	18.0	19.9	> 20 min	> 20 min
165	624.3	14.5	21.9	2,3 min	> 20 min
300	176.7	4.6	8.3	50 s	4.5 min
340	56.9	2.6	3.4	30 s	1.8 min
400	15.8	1.2	2.5	18 s	20 s
ZnO MOS sensor					
75	-	-	-	-	-
165	-	-	-	-	-
300	14.3	0.7	1.1	1.2 min	1.8 min
340	22.8	0.8	1.5	50 s	1.8 min
400	38.6	1.2	1.8	20 s	1.2 min

(-) No response towards investigated gaseous mixture.

* The gas responses at 75°C present a very slow response time and the normalized response is measured before the complete resistance variation is reached, this value is therefore a transitory one and is under-evaluated.

The $K_{CO/NH3}$ coefficient was also improved as compared to the ZnO sensor ($K_{CO/NH3}$=1.8 at 400°C). Since, the CuO sensor is not sensitive to NH_3 at all, the $K_{CO/NH3}$ for this sensor is higher than for the CuO(75%)/ZnO(25%) one.

The response time of the CuO(75%)/ZnO(25%) sensor to 100 ppm CO at 165 °C is quite long (t_{90}=2.3 min) but shorter than for the CuO one (t_{90}=6.2 min at 165 °C) (Table 2). Unfortunately, at this temperature the recovery is very slow, *i.e.* t_{10} > 20 minutes (Fig. 5a). Therefore, to shorten the analysis time it is better to operate at 300°C. Even if, for these conditions, the sensor exhibits lower sensitivity (S_{CO} = 177%) and selectivity ($K_{CO/C3H8}$ = 4.7 and $K_{CO/NH3}$ = 9,8), the response/recovery time is significantly shortened (t_{90} = 50 s, t_{10} = 4.5 min) (Fig. 5b). It is noteworthy, however, that at 300 °C, the CuO(75%)/ZnO(25%) sensor still presents better sensitivity and selectivity than the devices based on pure CuO (S_{CO}=2 3%, $K_{CO/C3H8}$ =2.9 at 300 °C) or ZnO (S_{CO}=14 %, $K_{CO/C3H8}$ =0.67 and $K_{CO/NH3}$=1.1 at 300 °C) sensitive layers.

Sensitivity and response/recovery time are closely related to the sensor operating temperature. At low temperature the adsorption is favored, with the

formation of strong chemical bonds between the analyzed gas and the surface of the sensitive metal oxide semiconudctor layer. This enhanced interaction increases the change in sensor resistance and thus its sensitivity. However, at such low temperature, the process of gas diffusion in the material and its desorption process are less efficient, negatively affecting other sensor parameters (*e.g.* recovery/regeneration time). Of course, as the temperature increases, the increased thermal movement of the gaseous molecules can be observed, leading to an increase in the desorption rate, which, in turn, may reduce the sensitivity of the sensor [24].

Data described above are in agreement with results published earlier. Indeed, several CuO-ZnO based sensors have been described for selective and sensitive detection of HCHO, C_3H_6O, C_2H_5OH, NO_2, CO_2, H_2S or NH_3 [12-18]. These results showed that the ZnO/CuO heterojunction sensors exhibits higher sensitivity, better selectivity and shorter response/recovery time than the devices based on single oxides (Table 3).

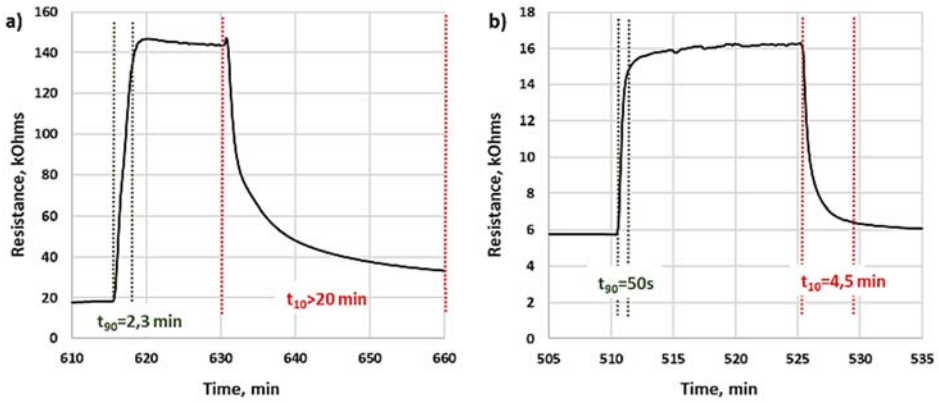

Fig. 5. Response of the CuO(75%)/ZnO(25%) MOS sensor at 165ºC (a) and 300ºC (b) towards 100 ppm of CO

Table 3. Examples of ZnO / CuO based gas sensors

Sensing material	T_{op}	Target gas	Gas conc.	S (%)*	$t_{(90)}/t_{(10)}$	Comments	Ref
CuO nanoparticles/ ZnO nanoparticles	225°C	H_2S	1 ppm	800%	30/100s	Stronger and faster response as compared to CuO and ZnO nanoparticle sensors	[12]
ZnO nanorods/ CuO nanoparticles	RT	NH_3	1 ppm	159%	2,3/2,1s	Better sensitivity and selectivity as compared to ZnO and CuO sensors	[13]
ZnO / CuO nanorods	RT	CO_2	1000 ppm	9,7%	4.2/3,5 min	Sensor is not sensitive to environmental gases such as CO, NO_2 and H_2S.	[14]
ZnO nanowires/ CuO nanoparticles	150°C	NO_2	100 ppm	175%	14 /197s	Low sensitivity (below 20%) towards CH_3OH, SO_2, CO, H_2S, Cl_2	[15]
CuO@ZnO microcubes	240°C	C_2H_5OH	50 ppm	360%	5/18s	CuO@ZnO cubes offer 2.6 times higher response as compare to CuO sensor.	[16]
ZnO hexagonal prisms/ CuO nanoparticles	RT	HCHO	1 ppm	188%	1,78/2,9s	The ratio of CuO and ZnO in the sensitive layer influences greatly its performance	[17]
ZnO branched p-CuxO@n-ZnO nanowires	250°C	C_3H_6O	50 ppm	85%	-	The nanocomposite exhibits 6 times higher response as compare to CuO nanowires.	[18]
ZnO / CuO anisotropic nanoparticles	165°C	CO	100 ppm	624%	3s/20min	The ratio of CuO and ZnO in the sensitive layer influences greatly its performance	This work

* In this work the sensitivity is expressed as $S=(R_{air}-R_{gas})/R_{air}*100$. However, the sensitivity can be calculated in different ways, *i.e.* $S=R_{air}/R_{gas}$, $S=R_{gas}/R_{air}$, $S=(R_{air}-R_{gas})/R_{air}$, etc. Therefore, in some cases presented in the table we estimated the normalized response using response curves or data provided within the cited papers. This allows a better comparison of sensitivity parameter between different studies.

3.3. Gas Sensing Behavior

The response of the CuO and CuO/ZnO MOS sensors to reducing gas mixtures shows p-type sensing behavior. For p-type MOS sensors, the widely accepted gas sensing mechanism is based on the change of conductivity due to the interactions between the surface adsorbed oxygen species and the analyzed gas [25]. When CuO sensing layer is exposed to the air atmosphere, oxygen molecules will adsorb on its

surface to form oxygen species, and then captured free electrons of CuO to form a hole accumulation layer (HAL). When exposed to the CO, the gas molecules react with pre-adsorbed oxygen species on the CuO surface and return the captured electrons back to the conduction band (CB) of CuO. Meanwhile, the thickness of the HAL becomes thinner, and the resistance of the CuO increases.

According to previous reports [26, 27], the improvement of the gas sensing properties of p-type semiconductors combined with n-type semiconductors can be described as follows. When the CuO contacts in air with the ZnO, an internal self-built electrical field at the interface will be formed *via* charge carries diffusion due to their different work functions, electron affinities and band gaps. In the electrical field, the electrons transfer from ZnO to CuO, and holes move in the opposite direction until the systems achieve equalization at the Fermi level (E_F), as displayed on the Fig. 6a. The process will lead to development of the potential barrier at the heterojunctions as the band bending and a wide depletion layer appears at the interface.

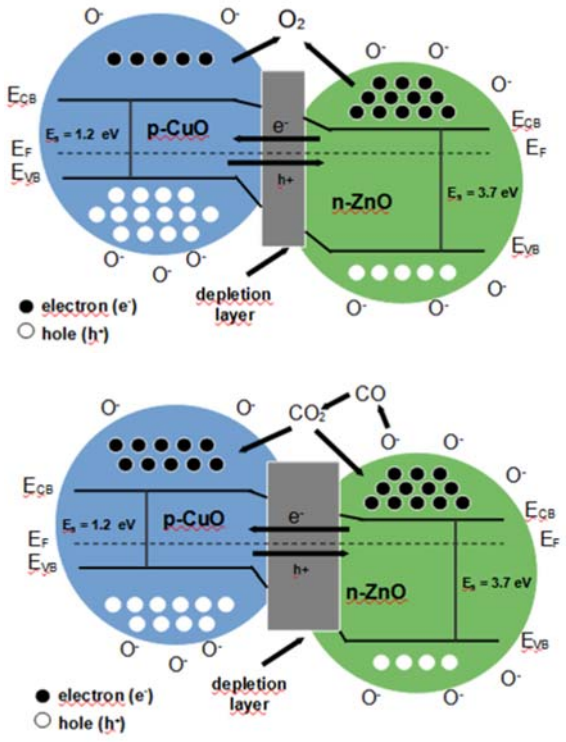

Fig. 6. The band diagram of the ZnO/CuO heterojunction (a) in the air (RH 50 %); (b) in the CO.

When the reducing gas is injected in, its molecules react with pre-adsorbed oxygen species and the electrons return back to the interfaces of the CuO and ZnO. The electrons return to the CB of the CuO and combine with the holes in the valence band (VB), which reduces the hole concentration in the CuO HAL and increases the resistance of CuO. On the other side, the electrons that have returned to the ZnO increase the electron concentration in the ZnO layer. The electrons transfer from ZnO to CuO until a new equilibrium is obtained (Fig. 6b). As a result, the hole quantity in the VB of the CuO is further reduced, which greatly increases the resistance of the CuO. This results in a significant improvement in the response of the CuO/ZnO gas sensor.

Taking into account the results obtained in this work, it is obvious that the CuO(75%)/ZnO(25%) sensor exhibits the highest number of heterojunctions. With increasing amount of the ZnO nanoparticles within the sensitive layer the amount of heterojunctions decreases and thus, the sensitivity decreases as well reaching the lowest values for the CuO(25%)/ZnO(75%) sensor. Moreover, at 340 °C the sensor does not respond (or the response is very week). The signal generated by the n-type ZnO is balanced by the response produced by the p-type CuO and CuO/ZnO heterojunction. A change from a p-type to n-type sensing behavior is thus observed (Fig. 4). Such transition has been observed before [28-31]. For example, temperature driven p- to n- type switching was described by Sinha et al. for sensitive layers made of CNT/ZnO composite [28]. Indeed, the CNT/ZnO composite is able to operate as a dual mode sensor, in which CNT dominates in mild temperature region (≤ 150 °C) and ZnO at high temperature region (>150 °C) with sensitivity of 72.6 % and 23.2 %, respectively.

4. Conclusions

The ZnO and CuO anisotropic nanoparticles and their mixtures were deposited on miniaturized gas sensors substrates as gas sensitive layers and exposed to different reducing gases (CO, C_3H_8, NH_3). Several conclusions can be drawn from these investigations:

- The ratio of ZnO and CuO nanoparticles within the sensitive layer play a crucial role on MOS sensor performances;
- The CuO(75%)/ZnO(25%) sensor exhibits the highest sensitivity and selectivity towards CO from all investigated sensors;
- Although the CuO(75%)/ZnO(25%) sensor can operate at relatively low temperature (165 °C), its recovery is very slow;
- The analysis time can be shorten by increasing the temperature up to 300 °C, but this will decrease the sensitivity and selectivity of the CuO(75%)/ZnO(25%) sensor;
- The enhanced gas sensing properties of CuO(75%)/ZnO(25%) sensor is attributed to the formation of the p-n heterojunction and its gas sensing mechanism is described;
- The CuO(25%)/ZnO(75%) sensor exhibits the lowest gas sensing performance towards tested gases,
- A shift from p-type to n-type sensing behavior is observed for the CuO(25%)/ZnO(75%) at 340 °C / 400 °C.

These results highlight the influence of the ZnO/CuO heterojunction on gas sensor sensitivity and selectivity, as well as on its response and recovery times. The CuO(75%)/ZnO(25%) sensor is a suitable candidate for an efficient CO sensing in the presence of C_3H_8 and NH_3.

Acknowledgements

This project has received funding from the European Union's Horizon 2020 research and innovation programme under the Marie Skłodowska-Curie grant agreement No 101033564. This work was partly supported by LAAS-CNRS micro and nano technologies platform member of the French RENATECH network.

References

[1]. M. V. Nikolic, V. Milovanovic, Z. Z. Vasiljevic, Z. Stamenkovic, Semiconductor Gas Sensors: Materials, Technology, Design, and Application, *Sensors,* 20, 2020, 6694.

[2]. B. Szulczyński, J. Gębicki, Currently Commercially Available Chemical Sensors Employed for Detection of Volatile Organic Compounds in Outdoor and Indoor Air, *Environments,* 4, 2017, 21.

[3]. Yaqoob, U., Younis, M. I., Chemical Gas Sensors: Recent Developments, Challenges, and the Potential of Machine Learning—A Review, *Sensors,* 21, 2021, 2877.

[4]. S. Sharma and M. Madou, A new approach to gas sensing with nanotechnology, P*hilosophical Transactions: Mathematical, Physical and Engineering Sciences,* 370, 2012, pp. 2448–2473.

[5]. M. L. Kahn et al., Size- and Shape-Control of Crystalline Zinc Oxide Nanoparticles: A New Organometallic Synthetic Method, *Adv. Funct. Mater*, Vol. 15, Issue 3, 2005, pp. 458-468.

[6]. G. Casterou, V. Collière, P. Lecante, Y. Coppel, P. A. Eliat, F. Gauffre, M. L. Kahn, Improved Transversal Relaxivity for Highly Crystalline Nanoparticles of Pure γ-Fe_2O_3 Phase, *Chemistry*, 14, 2015, pp. 18855-18861.

[7]. A. Ryzhikov et al., Organometallic synthesis of ZnO nanoparticles for gas sensing: towards selectivity through nanoparticles morphology, *Journal of Nanoparticle Research*, 17, 2015, 280.

[8]. J. Jońca et al., Organometallic Synthesis of CuO Nanoparticles: Application in Low-Temperature CO Detection. *ChemPhysChem,* Vol. 18, Issue 19, 2017, pp. 2658-2665.

[9]. J. Jońca et al., SnO_2 "Russian Doll" Octahedra Prepared by Metalorganic Synthesis: A New Structure for Sub-ppm CO Detection, *Eur. J. Chem.,* Vol. 22, Issue 29, 2016, pp. 10127-10135.

[10]. V. S. Bhati, M. Kumar, R. Banerjee, Gas sensing performance of 2D nanomaterials/metal oxide nanocomposites: a review, *Journal of Materials Chemitry C*, 9, 2021, pp. 8776-8808.

[11]. L. Liu, Y. Wang, Y. Liu, S. Wang, T. Li, S. Feng, S. Qin and T. Zhang, Heteronanostructural metal oxide-based gas microsensors, *Microsystems & Nanoengineering,* 8, 2022, 85.

[12]. S. Park, S. Kim, H. Kheel, S. K. Hyun, C. Jin, C. Lee, Enhanced H_2S gas sensing performance of networked CuO-ZnO composite nanoparticle sensor, *Materials Research Bulletin*, Vol. 82, October 2016, pp. 130-135.

[13]. C. Cheng, C. Chena, H. Zhang, Y. Zhang, Preparation and study of ammonia gas sensor based on ZnO/CuO heterojunction with high performance at room temperature, *Materials Science in Semiconductor Processing*, Vol. 146, 2022, 106700.

[14]. S. Keerthana, K. Rathnakannan, Hierarchical ZnO/CuO nanostructures for room temperature detection of carbon dioxide, *Journal of Alloys and Compounds*, Vol. 897, 2022, 162988.

[15]. Y. H. Navale, S. T. Navale, F. J. Stadler, N. S. Ramgir, V. B. Patil, Enhanced NO_2 sensing aptness of ZnO nanowire/CuO nanoparticle heterostructure-based gas sensors, *Ceramics International,* 45, Issue 2, Part A, 2019, pp. 1513-1522.

[16]. M. Yin, F. Wang, H. Fan, L. Xu, S. Liu, Heterojunction CuO@ZnO microcubes for superior p type gas sensor application, *Journal of Alloys and Compounds,* Vol. 672, 2016, pp. 374-379.

[17]. J. Liu, Y. Chen and H. Zhang, Study of Highly Sensitive Formaldehyde Sensors Based on ZnO/CuO Heterostructure via the Sol-Gel Method, *Sensors,* 21, 14, 2021, 4685.

[18]. X.-T. Xue, L.-Y. Zhu, K.-P. Yuan, C. Zeng, X-X. Li, H.-P.Ma, H.-L. Lu, D. W. Zhang, ZnO branched p-CuxO @n-ZnO heterojunction nanowires for improving acetone gas sensing performance, *Sensors and Actuators B: Chemical,* Vol. 324, 2020, 128729.

[19]. Ph. Menini et al., High performances of new microhotplate for gas sensors, in *Proceedings of the 22nd European Conference on Solid state Transducers (EUROSENSORS XXII),* September 2008, Dresden, Germany, hal-02099850.

[20]. Microdrop Technologies: http://www.microdrop.de/wDeutsch/technology/microdrop.shtml?navid=28

[21]. Z. Zhao, Z. Zheng, C. Roux, C. Delmas, J.-D. Marty, M. L. Kahn, C. Mingotaud, Importance of the Correlation between Width and Length in the Shape Analysis of Nanorods: Use of a 2D Size Plot To Probe Such a Correlation, *Chemistry - A European Journal*, Vol. 22, Issue 35 2016, pp. 12424-12429.

[22]. A. A. Radhakrishnan, B. B Beena, Structural and Optical Absorption Analysis of CuO Nanoparticles, *Indian Journal of Advances in Chemical Science,* 2, 2, 2014, pp. 158-161.

[23]. M. El-Kemary, H. El-Shamy, I. El-Mehasseb, Photocatalytic degradation of ciprofloxacin drug in water using ZnO nanoparticles, *Journal of Luminescence,* 130, 2, 2010, pp. 2327-2331.

[24]. N. A. Isaac, I. Pikaar, G. Biskos, Metal oxide semiconducting nanomaterials for air quality gas sensors: operating principles, performance, and synthesis techniques, *Microchimica Acta,* 189, 2022, 196.

[25]. H. J. Kim, J. H. Lee, Highly sensitive and selective gas sensors using p-type oxide semiconductors: Overview. *Sensors and Actuators B*, 192, 2014, pp. 607-627.

[26]. H. Zhang, H. Li, L. Cai, Q. Lei, J. Wang, W. Fan, K. Shi, G. Han, Performances of In-doped CuO-based heterojunction gas sensor, *Journal of Materials Science: Materials in Electronics*, 31, 2020, pp. 910-919.

[27]. L. Cai, H. Li, H. Zhang, W. Fan, J. Wang, Y. Wang, X. Wang, Y. Tang, Y. Song. Enhanced performance of

the tangerines-like CuO-based gas sensor using ZnO nanowire arrays, *Materials Science in Semiconductor Processing*, Vol. 118, 2020, 105196.

[28]. M. Sinha S. Neogi, R. Mahapatra, S. Krishnamurthy, R. Ghosh, Material dependent and temperature driven adsorption switching (p- to n- type) using CNT/ZnO composite-based chemiresistive methanol gas sensor, *Sensors and Actuators B: Chemical,* 336, 2021, 129729.

[29]. R.-C. Wang, Y.-R. Hou, J.-Y. Liu, and Y.-W. Chen, Differentiating Ammonia from Other Reducing Gases via Response Reversal Phenomena by Varied ZnO/CuxO Nanorod Arrays, *Journal of the Electrochemical Society*, 165, 2018, B484.

[30]. X. Zhou, T. Tao, Y. Bao, X. Xia, K. Homewood, Z. Wang, M.Lourenço, Z. Huang, G. Shao, and Y. Gao, Dynamic Reaction Mechanism of P–N-Switched H_2-Sensing Performance on a Pt-Decorated TiO_2 Surface, *ACS Applied Materials and Interfaces* 13, 21, 2021, pp. 25472–25482.

[31]. S. Rani, M. Kumar, P. Garg, R. Parmar, A. Kumar, Y. Singh, V. Baloria, U. Deshpande, and V. N. Singh, Temperature-Dependent n–p–n Switching and Highly Selective Room-Temperature n-$SnSe_2$/p-SnO/n-SnSe Heterojunction-Based NO_2 Gas Sensor, *ACS Applied Materials and Interfaces*, 14, 13, 2022, pp. 15381–15390.